A kinesin5, Cin8, recruits protein phosphatase 1 to kinetochores and regulates chromosome segregation

Aussie Suzuki[#,1,3,6,*], **Amitabha Gupta**[#,2], **Sarah K Long**[1], **Rena Evans**[2], **Benjamin L. Badger**[1], **Edward D. Salmon**[1,5], **Sue Biggins**[2,5,*], and **Kerry Bloom**[1,5]

[1]Department of Biology, University of North Carolina at Chapel Hill, Chapel Hill, NC 27599, USA

[2]Howard Hughes Medical Institute, Division of Basic Sciences, Fred Hutchinson Cancer Research Center, Seattle, WA 98109, USA

[3]McArdle Laboratory for Cancer Research, Department of Oncology, School of Medicine and Public Health, University of Wisconsin-Madison, Madison, WI 53705, USA

[5]These authors jointly supervised this work

[6]Lead Contact

[#] These authors contributed equally to this work.

Summary

Kinesin-5 is a highly-conserved homo-tetrameric protein complex, responsible for crosslinking microtubules and pushing spindle poles apart. The budding yeast kinesin-5, Cin8, is highly concentrated at kinetochores in mitosis before anaphase, but its functions there are largely unsolved. Here, we show that Cin8 localizes to kinetochores in a cell cycle-dependent manner and concentrates near the microtubule binding domains of Ndc80 at metaphase. Cin8's kinetochore localization depends on the Ndc80 complex, kinetochore microtubules, and the Dam1 complex. Consistent with its kinetochore localization, a Cin8 deletion induces a loss of tension at the Ndc80 microtubule binding domains and a major delay in mitotic progression. Cin8 associates with PP1 (Protein Phosphatase 1) and mutants that inhibit its PP1 binding also induce a loss of tension at the Ndc80 microtubule binding domains and delay mitotic progression. Taken together, our results suggest that Cin8-PP1 plays a critical role at kinetochores to promote accurate chromosome segregation by controlling Ndc80 attachment to microtubules.

Introduction

To ensure accurate chromosome segregation, spindle microtubules attach to the specific region of the chromosome called the kinetochore. The kinetochore is a macro-molecular protein complex containing more than 100 proteins that assembles on a specialized centromeric chromatin structure [1, 2].

The highly conserved Ndc80 complex has critical functions in mediating microtubule attachment and force generation, as well as controlling the spindle assembly checkpoint, the surveillance mechanism that prevents anaphase until all kinetochores are properly attached to spindle microtubules [1, 3–6]. The Ndc80 complex binds to microtubules via two adjacent domains: a CH domain and an N-terminal tail. Microtubule binding affinity is regulated by phosphorylation and dephosphorylation of the tail domain in response to the dominance of either the kinase or phosphatase [7–11]. During prometaphase, phosphorylation by Aurora B kinase dominates, weakening the interaction between Ndc80 and kinetochore microtubules in order to allow correction of attachment errors. In contrast, during metaphase, dephosphorylation by the Protein Phosphatase 1 (PP1) dominates to strengthen Ndc80 attachments to kinetochore microtubules [10]. In budding yeast, deletion of the N-terminal tail results in loss of tension at the Ndc80 microtubule interface as measured by a FRET tension biosensor within Ndc80 [4]. Other important kinetochore-bound yeast Microtubule Associated Proteins (MAPs) are the Dam1 complex and Stu2/ch-TOG, which are both recruited to kinetochores via Ndc80. The Dam1 complex contributes to kinetochore microtubule attachment by oligomerizing into a ring-like structure that surrounds a microtubule *in vitro* [12–19]. Stu2, which is a microtubule polymerase, also binds the Ndc80 complex [20–22]. Recent studies show that Ndc80, the Dam1 complex, and Stu2 work together at kinetochores to share the load for chromosome segregation in budding yeast [4, 5, 21, 23, 24].

In addition to kinetochore-bound MAPs, cytoskeleton motor proteins also have critical roles in chromosome segregation in most eukaryotic cells. Kinesin-5, also known as Eg5 or KIF11 in vertebrates, is a highly conserved homotetramer protein complex with two-pairs of motor domains oriented in an opposite direction that serves to cross-link and slide anti-parallel microtubules apart [25, 26]. There are two Kinesin-5 family members in budding yeast: Cin8 and Kip1 [26, 27]. Unlike Kinesin-5 proteins in other species, Cin8 can behave as a bi-directional kinesin depending on whether it works alone or in conjunction with a team [28, 29]. Cin8 concentrates on central spindle microtubules during anaphase and plays a critical role in the maintenance of spindle pole separation [27, 30]. Although Cin8 and Kip1 are functionally redundant for bipolar spindle formation, Cin8 makes a greater contribution to chromosome segregation [27, 31]. *cin8* cells are viable at 25 °C, but they have a high rate of chromosome loss and prolonged progression through mitosis [27, 30]. Unlike *kip1* cells, *cin8* cells are synthetically lethal with inactivation of the spindle assembly checkpoint, suggesting a critical role in the segregation process [32]. Cin8 has been reported to bind to kinetochores based on a CEN DNA ChIP (Chromatin Immunoprecipitation) assay and fluorescence localization [31, 33]. However, previous studies have mainly focused on the microtubule motor functions of Cin8 [26, 28, 29, 31] and the functions of Cin8 at kinetochores have been largely unsolved.

Here, we demonstrate that Cin8 localizes to kinetochores in a cell cycle dependent manner, achieving maximum concentration at kinetochores prior to anaphase. Cin8 localization to the kinetochore depends on the Ndc80 complex, kinetochore microtubules, and the Dam1 complex. Cin8 directly binds to the Dam1 complex *in vitro* and associates with PP1 through a consensus PP1 binding motif. Depletion of Cin8 leads to a delay in mitotic progression that is associated with the loss of tension at Ndc80 microtubule binding domains as measured by the Ndc80 tension biosensor. Similar defects are produced by mutation of the Cin8 PP1 binding motif, although its kinetochore localization is normal. These defects are almost as severe as those in cells lacking the N-terminal tail of Ndc80 [4, 34]. Our results demonstrate that a PP1/Cin8 complex plays a critical role in producing the tension needed at the Ndc80 microtubule binding domains to ensure normal mitotic progression and accurate chromosome segregation.

Results

Cin-8 localizes to kinetochores in cell cycle-dependent manner

To better understand the localization of Cin8 to kinetochores, we measured its concentration at kinetochores throughout the cell cycle by quantitative light microscopy. The concentration of Cin8 on kinetochores was greatest at metaphase, significantly reduced in anaphase to approximately 20% of metaphase levels, and partially recovered during interphase (Figure 1A). Consistent with this, Cin8 co-immunoprecipitated with kinetochores via Dsn1 (Figure 1B, left), a core kinetochore protein that is a component of the Mis12 complex/MIND complex and allows for the isolation of native kinetochores [35] (See details in [21, 36, 37]). The levels of co-immunoprecipitated Cin8 were highest at ~70-101 min after α-factor release, when the cells were highly enriched at metaphase (Figures 1B, right, and S1A). To test whether the kinetochore localization of Cin8 requires microtubules, we measured Cin8 levels after nocodazole treatment, a microtubule depolymerizing drug. Nocodazole-treatment induced an 80% reduction of Cin8 at kinetochores as well as a ~90% reduction of microtubules compared to control (Figure 1C). We also examined Cin8 levels on purified kinetochores after nocodazole-treatment and found they were significantly reduced compared to control (Figure 1D). Interestingly, a low dose treatment of benomyl, which induces loss in the extent of microtubule dynamic instability (dynamicity) as well as a ~50% reduction of microtubules due to preferential depolymerization of non-kinetochore microtubules [4, 38], did not affect the levels of Cin8 at kinetochores (Figure 1C). These results indicate that Cin8 localizes at the kinetochore from early mitosis through metaphase, and its kinetochore localization requires kinetochore microtubules, but it does not require the normal level of kinetochore microtubule dynamicity nor the normal concentration of non-kinetochore spindle microtubules.

The core structural kinetochore proteins including the Ndc80 complex, Dam1 complex, and CCAN (constitutive centromere associated protein network) proteins, are stably associated with kinetochores during metaphase [39]. To test if Cin8 is also stably associated with kinetochores, we analyzed the turnover rate of Cin8-GFP using fluorescence recovery after photobleaching (FRAP). The half-life for fluorescence recovery after photo-bleaching of

kinetochore Cin8-GFP was ~35-40 sec (Figures. S1B-C). Thus, Cin8 is a dynamic component of the kinetochore, unlike the core-structural proteins.

Cin8-Dam1 interaction promotes Cin8 kinetochore localization

Next, we more specifically investigated the location of Cin8 relative to the kinetochore Ndc80 complex. We determined the positions of the C-terminus of Cin8 and the C-terminus of Ndc80 relative to the Spindle Pole Body (Spc29) by fluorescence co-localization. The mean position of the C-terminus of Cin8 localized outside (toward to pole) of the mean position of the C-terminus of Ndc80, near the expected position of the N-terminus of Ndc80 (Figure 2A) [40, 41]. From this localization result, we hypothesized that Cin8 may interact with the proteins located near the N-terminus of the Ndc80 complex, such as the Ndc80 and the Dam1 complexes. To test this hypothesis, we analyzed Cin8 levels at kinetochores in cells depleted of Ndc80 or Dam1 by a quantitative LM method (Figure 2B). The Ndc80 and Dam1 proteins were fused at the endogenous locus to the auxin-inducible degron (AID) epitope tag to mediate degradation of the corresponding proteins in the presence of auxin and the F box protein OsTir1 [42]. There was a significant decrease in Cin8 levels at the kinetochore in both strains, so we further examined this by purifying kinetochores from cells containing temperature sensitive mutants in the Ndc80 and Dam1 complex (*ndc80-1* and *dad1-1*, respectively). To ensure that cells were at similar cell cycle stages, the kinetochores were purified from cells arrested in metaphase prior to the temperature shift. Consistent with the microscopy data, the levels of co-immunoprecipitated Cin8 were less than 10% of control in *ndc80-1* mutant cells and significantly reduced in *dad1-1* cells (a member of the Dam1 complex) (Figure 2C). Because inactivating Ndc80 induces the loss of proteins associated with Ndc80, including the Dam1 complex [15, 19, 43, 44], we tested whether Cin8 interacts directly with Ndc80 or Dam1 complexes by performing *in vitro* binding assays. The Ndc80 complex or Dam1 complex was immobilized on beads (see [21] for methods) and increasing amounts of purified Cin8 were added. There was a dose-dependent increase in the amount of Cin8 that bound to the Dam1 complex but not to Ndc80, indicating that Cin8 directly associates with the Dam1 complex (Figure 2D). Taken together, these results suggest that the Dam1 complex is a receptor for Cin8 at the kinetochore. However, there is still some Cin8 on kinetochores purified from cells lacking Dam1, suggesting there may be one or more additional Cin8 receptors at the kinetochore *in vivo*. Because this residual localization is abolished when Ndc80 is mutated, it is possible that Ndc80 is required for the localization of all Cin8 receptors or that the defect in microtubule attachments in *ndc80* mutants prevents Cin8 from localizing to kinetochores.

Cin8 is essential for proper mitotic progression and tension at the microtubule binding domains of Ndc80.

In order to investigate the functions of Cin8 at the kinetochore, we measured mitotic duration by time-lapse imaging in cells where Cin8 was deleted. *cin8* cells were severely delayed between prometaphase and anaphase onset in addition to the earlier reported significant delay in anaphase progression (Figure 3A) [30]. We previously found that tension at the microtubule binding domains of Ndc80 is essential for proper mitotic progression [4]. To examine whether loss of *CIN8* affects mitotic progression due to a lack of tension at the Ndc80 microtubule binding domains, we analyzed Ndc80 tension in *cin8* cells using the

Ndc80 tension sensor [4]. Cells lacking Cin8 had a significant loss of tension at the Ndc80 microtubule binding domains as revealed by higher FRET emission ratios compared to controls in prometaphase and metaphase, when Cin8 strongly localizes at kinetochores (Figure 3B). The mean values of FRET emission ratio in *cin8* cells at prometaphase and metaphase were near 3.8 and 3.4, respectively. These values are close to the values of zero tension in the FRET sensor as measured by *in vitro* and *in vivo* experiments [4] indicating that Cin8 is essential for producing proper tension at the microtubule binding domains of Ndc80.

We then asked what causes the loss of this Ndc80 tension in *cin8* cells. A previous study reported that the protein copy numbers of the Ndc80 and Dam1 complexes as well as microtubule dynamicity are critical to induce proper tension at Ndc80 [4]. We therefore examined the kinetochore levels of Ndc80 and Nuf2 (another component of the Ndc80 complex) in *cin8* cells at metaphase and found they were similar to control cells (Figure S2A). Next, we measured the levels of three components in the Dam1 complex at kinetochores in *cin8* cells and found no significant difference for Dad1, Dad3, and Ask1 protein levels compared to control cells (Figure S2B). There was also no significant difference in the stoichiometry of core structural kinetochore components when purified kinetochores were examined by silver-stained PAGE (Figure S2C) [5, 21, 37]. Lastly, we examined the degree of microtubule dynamicity by FRAP, but did not detect significant differences in the rates of FRAP between control and *cin8* cells (Figure S2D). As expected [38], WT cells treated with a low dose of benomyl exhibited a severe delay in microtubule fluorescence recovery (Figure S2D). These results imply that Cin8 is involved in controlling tension at the microtubule binding domains of Ndc80 without changing microtubule dynamicity or the amount of Ndc80 and Dam1 complexes at kinetochores.

The N-terminal tail of Ndc80 is required to generate tension [4], and we noticed that the phenotypes of the *cin8* cells are very similar to those in an Ndc80 mutant lacking the tail (Ndc80 tailless) (Figures 3A-B) [4, 30, 34]. To determine whether Cin8 might act through the Ndc80 tail, we constructed cells lacking both Cin8 and the tail domain of Ndc80 and examined their phenotype. There was no additional mitotic delay in the double mutant cells (Figure S3A), suggesting that Cin8 may be involved in tension control at the N-terminal tail of Ndc80. The N-terminal tail of Ndc80 is not responsible for recruiting Cin8 to kinetochores since Cin8 levels at kinetochores did not change in Ndc80 tailless mutant cells compared to control (Figure S3B).

Cin8 recruits PP1 to mediate proper mitotic progression and tension at Ndc80

The affinity of the Ndc80 tail for microtubules is regulated by the degree of phosphorylation, which is mediated by the balance of Aurora B kinase activity and the opposing PP1 phosphatase [4, 9–11, 23]. When kinetochores establish bi-oriented attachments at metaphase, Ndc80 should be dephosphorylated by PP1 to increase its affinity for kinetochore microtubules to generate maximal force production [10, 45]. Because Cin8 depletion did not alter the loss of Ndc80 tension exhibited by the Ndc80 tailless, we hypothesized that Cin8 may contribute to dephosphorylation of the Ndc80 tail to enhance microtubule binding affinity. PP1 opposes Aurora B phosphorylation, so we tested whether

Cin8 associates with PP1 by a co-immunoprecipitation assay. Indeed, the catalytic subunit of PP1, Glc7, co-purified with Cin8 (Figure 4A). To determine whether the association is through direct binding to Cin8, we analyzed Cin8 for PP1 binding motifs and found two conserved binding motifs (Figure 4B); one (RVKW) is in the unstructured region between coiled-coils 3 and 4, and another (RVDF) is in coiled-coil 2, which is unlikely to bind to PP1 because it associates with unstructured regions. We therefore made mutants in the RVKW motif to abolish Glc7 binding (*cin8-KAAKA or cin8-RAKA*). As a control, we also constructed *cin8-F467A*, a mutant in the Cin8 motor domain that decreases its microtubule binding affinity (~10 times lower than wild-type Cin8 *in vitro*) [46]. We tested whether the mutants altered the levels of PP1 that co-immunoprecipitate with Cin8. While the amounts of Glc7 that co-purified with wild-type Cin8 and the *cin8-F476A* were similar, there was a significant decrease in the amount that co-purified with the *cin8-KAAKA* (Figure 4C). We next asked whether Cin8 contributes to the kinetochore localization of PP1 by isolating kinetochores via immunoprecipitation of Dsn1 from cells expressing wild-type Cin8, *cin8-KAAKA* or *cin8-F476A*. While PP1 levels on the kinetochore were similar to cells expressing Cin8 or the *cin8-F476A*, they were almost abolished in the *cin8-KAAKA* (Figure 4D). Taken together, these results suggest that Cin8 associates with Glc7/PP1 through its PP1 binding motif (RVKW) at the C-terminus, and this helps to recruit PP1 to the kinetochore.

We next asked if a decrease in PP1 at kinetochores is responsible for the severe mitotic delay observed in Cin8 deletion cells by characterizing the phenotypes of the PP1 binding mutant. WT, *cin8*, and *cin8-RAKA* strains were analyzed for the percentage of cells in prometaphase and metaphase by microscopy (Figure 4E). There was a significant increase in cells delayed in mitosis in both *cin8* mutant strains, consistent with a role for PP1 binding in mediating mitotic progression. To determine whether this delay is associated with a lack of tension at Ndc80, we examined whether the *cin8-RAKA* cells have lost tension at the microtubule binding domains of Ndc80 using the Ndc80 tension biosensor. The FRET emission ratio at metaphase was significantly higher (~3.3) in *cin8-RAKA* cells compared to control (~2.2), indicating almost complete loss of tension as occurs with *cin8* cells and Ndc80 tailless mutants (Figures 3B and 4F) [4]. We note that the *cin8-RAKA* cells did not alter the level of Cin8 at kinetochores (Figure S3C). These results show that recruitment of PP1 to kinetochores by Cin8 is critical to ensure proper tension at Ndc80 microtubule binding domains and to achieve normal rate of progression through mitosis (Figure 4G).

Discussion

Cin8 was previously reported to associate with CEN DNA by a ChIP assay [33]. Here, we show that Cin8 purifies with kinetochores and localizes near the N-terminus of Ndc80 in a cell cycle regulated manner. We also found that there is a direct interaction between Cin8 and the Dam1 complex. This interaction likely facilitates the enrichment of Cin8 at kinetochores in addition to the interaction between Cin8 and kinetochore microtubules. Because Ndc80 recruits Dam1 to kinetochores, this also explains the lack of Cin8 localization to kinetochores in the *ndc80* and *dam1* mutant cells. However, further studies are required to reveal the detailed interaction between the Cin8 and the Dam1 complex as well as the contribution of motor activities in kinetochore localization.

A major finding of our study is that Cin8 controls both tension at Ndc80 microtubule binding domains and the rate of progression through mitosis by recruiting PP1 to the kinetochore (Figure 4G). We favor the possibility that PP1 bound to Cin8 contributes to the dephosphorylation of Ndc80, increasing microtubule binding affinity. This is because the phenotype of *cin8-RAKA* cells is similar to Ndc80 tailless, although both these mutants still exhibit the same level of Cin8 at the kinetochore as controls. However, we were not able to generate an Ndc80 tension sensor strain that also contains mutations in the 7 Aurora B phosphorylation sites to test whether it would restore tension in *cin8-RAKA* cells as predicted if Ndc80 were the key target. In addition, other kinetochore proteins such as Dam1 are regulated by PP1, so it will be important to precisely determine the direct targets of the Cin8-PP1 complex in the future.

Our results highlight Cin8 as a major recruiter of PP1 to kinetochores, but other proteins also contribute. The FRET emission ratio of the Ndc80 tension biosensor in *cin8* cells or *cin8-RAKA* mutants was slightly lower than the Ndc80 tailless. The Spc105/Knl1 protein is known to recruit PP1 to silence the spindle checkpoint [36, 47, 48], and it could also contribute to Ndc80 dephosphorylation. Given that there are multiple PP1 regulatory subunits at kinetochores, it was surprising that kinetochores purified from *cin8-KAAKA* mutant cells lacked detectable PP1 (Figure 4D). However, we note that these cells are delayed in mitosis by a lack of tension, so the Aurora B protein kinase will be active and phosphorylate Spc105 and possibly other regulatory subunits to inhibit PP1 association. Therefore, the lack of PP1 on kinetochores purified from *cin8-KAAKA* mutant cells may reflect a combination of multiple activities that contribute to PP1 localization. Nevertheless, Cin8 appears to be a significant PP1 recruiter based on the severity of loss in tension at the Ndc80 microtubule binding domains.

Kinesin-5 is highly conserved from yeast to human, but human Kinesin-5, Eg5, does not localize to kinetochores, in contrast to budding yeast Cin8. However, a recent study reports that the human kinesin-like protein Kif18a recruits PP1 to kinetochores [49]. Additional studies show that PP1 recruited by Kif18a is critical for dephosphorylation of the Ndc80 microtubule binding domains to stabilize microtubule attachment in HeLa cells [50]. This indicates that human Kif18a acts like Cin8 in budding yeast. Our study has discovered a critical positive-feedback regulatory pathway that promotes tension at the Ndc80 microtubule binding domains and normal mitotic progression, and this control mechanism might also be highly conserved process for accurate chromosome segregation in eukaryotic cells.

STAR METHODS

CONTACT FOR REAGENT AND RESOURCE SHARING

Further information and requests for resources and reagents should be directed to and will be fulfilled by the Lead Contact, Aussie Suzuki (aussie.suzuki@wisc.edu).

EXPERIMENTAL MODEL AND SUBJECT DETAILS

Yeast strains and cell preparation—All yeast strains are described in KEY RESOURCES TABLE and were generated by standard techniques. All yeast cells used for imaging were grown to logarithmic phase at 24 °C in rich YPD media. For benomyl or nocodazole treatment prior to imaging, we added 55 μM of benomyl for low concentration and 10 μM of nocodazole to logarithmic phase cells and incubated for 1 h at 24 °C. For biochemistry experiments, 10 μg/ml of nocodazole was added for 15 minutes or 1 hour prior to harvesting. For cell synchronization, alpha factor was added to 1 μg/ml of culture for 3 hours. At >90% arrest, an aliquot of cells was harvested and the remaining cells were washed 5× in equal volumes of YEP before resuspending in YEP. Cells were monitored for budding as an indication of the start of S-phase (~40 minutes). Equivalent volumes were harvested every 30 minutes and fixed or processed for protein purification.

METHOD DETAILS

Auxin Inducible Degradation—The auxin inducible degron (AID) system was used essentially as described in [51]. Briefly, cells expressed C-terminal fusions of the protein of interest to an auxin responsive protein (IAA7) at the endogenous locus. Cells also expressed Tir1, which is required for auxin-induced degradation. 500 μM IAA (indole-3-acetic acid dissolved in DMSO; Sigma) was added to media for 2 hours to induce degradation of the AID-tagged protein. In strains with *cdc20-AID*, strains were then shifted to 37 °C for 2 hours to inactivate the indicated temperature sensitive protein and an additional 500 μM IAA was added prior to harvesting.

Protein purification—Ndc80 was purified as described in [21]. Dam1 complex was purified similarly with the following modifications. Dad1 was C-terminally tagged at the endogenous locus with 3-Flag and the first wash was performed with BH/0.4M KCl. Buffer H (BH) contains 25 mM HEPES pH 8.0, 2 mM MgCl2, 0.1 mM EDTA, 0.5 mM EGTA, 0.1% NP-40, 15% glycerol with KCl at the indicated concentration. Cin8 was purified similarly with the following changes: Cin8 was either -3V5 tagged or -SNAP-3V5 tagged at the C-terminus. Cells were harvested and washed in BH/0.15 supplemented with 500 μM Mg-ATP. Following the IP, Cin8 was washed in either BH/0.15 for co-IP or BH/0.5 for pure protein supplemented with 100 μM Mg-ATP. The final wash and storage buffer for Cin8 was BH/0.15 supplemented with 50μM Mg-ATP. For binding experiments, Ndc80c or Dam1c were purified and immobilized on Flag beads. Freshly purified Cin8 was added in 1/3 serial dilutions to immobilized protein. Following 3 washes in BH/0.15 supplemented with 50 μM Mg-ATP, proteins were eluted with Flag peptide and run on a 4-12% gradient gel. Quantification of bound and unbound Cin8 was performed using a Typhoon and quantification of Ndc80 and Dam1c was estimated by analysis of silver stained PAGE gels with BSA protein standards.

Imaging (FRET)—Imaging was performed on a Nikon TE2000-E microscope equipped with a 100×/1.4NA (Planapo) DIC oil immersion objective. Images were recorded with MetaMorph 7.1 software (Molecular Devices) on an ANDOR iXON (DV897) EMCCD camera with a total magnification giving a pixel size of 106.7 nm with no electron multiplication. FRET and mECFP fluorescence images were obtained from a Dual-View 2

imaging device (Photometrics) with an 89002 ET-ECFP/EYFP filter (Chroma Technology). This allowed simultaneous imaging of both the FRET channel (CFP excitation, YFP emission) and the mECFP channel (CFP excitation, YFP emission). See details in [4].

Imaging (other)—Images were obtained sequentially at 200 nm steps along the z axis using Nikon Element software (Nikon), a Nikon Eclipse Ti microscope with image magnification yielding a 64 nm pixel size from a 100×/1.49NA (Apo TIRF) DIC oil immersion objective (Nikon) and an ANDOR Clara CCD camera (ANDOR). See details in [4].

Fluorescence intensity measurement—Fluorescent intensity measurement method is essentially as described in [4, 52]. The z-axis position of best focus (maximum integrated intensity) was used for the analysis of sister kinetochore clusters. A 7×7 pixel region (for FRET images and a 11×11 for other images) was centered on a cluster of sister kinetochores to obtain integrated fluorescence, whereas a 9×9 pixel (for FRET images and a 13×13 for other images) region centered on the 7×7 pixel region was used to obtain surrounding background intensity. Fi = integrated intensity for 7×7 region (integrated counts for the 9×9 region integrated counts for 7×7 region) × pixel area of the 7×7 region/(pixel area of the 9×9 region pixel area of a 7×7 region). Measurements were made with MetaMorph 7.1 analysis software (Molecular Devices) using the region measurements tool.

FRET emission ratio (FRET emission/mECFP emission)—Changes in tension at the Ndc80 FRET biosensor were monitored in live cells by measurement of the emission ratio (defined as: FRET channel emission (CFP excitation, YFP emission)/mECFP channel emission (CFP excitation, CFP emission)). The FRET emission and CFP emission were measured by the method described above. This is a standard method when the biosensor contains one donor and one acceptor fluorescent protein. Detailed explanations are in [4].

Kinetochore purifications—Kinetochores were purified using bead beating lysis as specified in [53]. Immunoblotting was performed with Commercial antibodies as follows: α-Flag, M2 (Sigma-Aldrich) 1:3,000; α-V5 (Invitrogen) 1:5,000 or α-GFP, JL-8 (Living Colors) 1:5,000.

QUANTIFICATION AND STATISTICAL ANALYSIS

Statistical Analysis—All data were expressed, as means ±SD. Statistical significance was determined using Student's t-test for comparison between two independent groups. *P < 0.05 was considered statistically significant.

KEY RESOURCES TABLE

REAGENT or RESOURCE	SOURCE	IDENTIFIER
Antibodies		
Flag M2	Sigma-Aldrich	F1804
V5	Invitrogen	2F11F7

REAGENT or RESOURCE	SOURCE	IDENTIFIER
GFP (JL-8)	Living Colors	632380
Yeast Strains		
AUS004; 473A (Mata Trp 63, Leu2 63, Ura3-52, His3 200, Lys2-8 1), Spc29-RFP: Hb, Ndc80-FRET 12aa (410 aa): Ura3	[4]	N/A
AUS032; AUS004, Cin8 :Kan	This study	N/A
AS1DCB410.1; 473A Cin8-x3GFP:His, Spc29-RFP:Hb	This study	N/A
KBY8023; YELO61C, Cin8-GFP:HisMX6, Ndc80-mCherry:Kan	This study	N/A
MAY8526; 473a, Nuf2GFP:His, Spc29-RFP:Hb	[41]	N/A
AUS061; MAY8526, Cin8 :Kan	This study	N/A
TUB1-GFP; 473A, Tub1-GFP	[38]	N/A
AUS063; TUB1-GFP, Cin8 :His	This study	N/A
KBY7999; 473A, Spc29-RFP: Hb	[38]	N/A
AUS099; KBY7999. Cin8-GFP: His	This study	N/A
KBY7367; 473A, Ndc80-GFP: Trp	[41]	N/A
AUS106; KBY7367, Cin8 :His	This study	N/A
KBY7316; 473A, Ask1-GFP:HIS3	[41]	N/A
AUS108; KBY7316, Cin8 :kan	This study	N/A
AUS149; AUS004, cin8-RAKA:His	This study	N/A
SBY8253; SBY3 (Mat a ade2-1 can1-100 bar1-1 trp1-1 his3-11 leu2-3,112 ura3-1), DSN1-6His-3Flag:URA3	This study	N/A
SBY12078; SBY3, DSN1-6His-3Flag:URA3 his3-11::ASK1-myc:HIS3	This study	N/A
SBY12464; SBY3, DAD1-3FLAG:TRP1	This study	N/A
SBY13733; SBY3, SPC24-3FLAG:TRP1	This study	N/A
SBY14244; SBY3, GLC7-3GFP:HIS3	This study	N/A
SBY15231; SBY3, CIN8-SNAP-3V5:KANMx6	This study	N/A
SBY15249; SBY3, CIN8-3V5:KanMX6	This study	N/A
SBY15770; SBY3, CIN8-3V5:HygMX6	This study	N/A
SBY15778; SBY3, DSN1-6His-3Flag:URA3 CIN8-SNAP-3V5:KANMx6 MTW1-CLIP:KANMx6	This study	N/A
SBY16507; SBY3, DSN1-6His-3Flag:URA3 CIN8-3V5:HygMX6	This study	N/A
SBY16513; SBY3, DSN1-6His-3Flag:URA3 CIN8-3V5:HygMX6 CDC20-AID:KanMX6, leu2-3, 112::pGPD1-OsTIR1:LEU2	This study	N/A
SBY16515; SYB3, DSN1-6His-3Flag:URA3 CIN8-3V5:HygMX6 CDC20-AID:KanMX6, leu2-3, 112::pGPD1-OsTIR1:LEU2 ndc80-1	This study	N/A
SBY16519; SBY3, Dsn1-6His-3Flag:URA3 CIN8-3V5:HygMX6 CDC20-AID:KanMX6, leu2-3, 112::pGPD1-OsTIR1:LEU2 dad1-1:KANMx6	This study	N/A
SBY17127; SBY3, Dsn1-6His-3Flag:URA3 his3-11::ASK1-myc:HIS3 cin8 ::KANMx6	This study	N/A
SBY17463; SBY3, CIN8-3V5:KanMX6 GLC7-3GFP:HIS3	This study	N/A
SBY17756; SBY3, DSN1-6His-3Flag:URA3 GLX7-3GFP:HIS3 cin8 ::KANMx6, ura3-1:pCIN8-CIN8-KAAKA-3V5:URA3	This study	N/A
SBY17805; SBY3, DSN1-6His-3Flag:URA3 GLC7-3GFP:HIS3 cin8 ::KANMx6 ura3-1:pCIN8-CIN8-3V5:URA3	This study	N/A
SBY17806; Dsn1-6His-3Flag:URA3 GLC7-3GFP:HIS3 cin8 ::KANMx6, ura3-1:pCIN8-cin8-F467A-3V5:URA3	This study	
Chemicals, Peptides, and Recombinant Proteins		
nocodazole	Sigma	M1404
benomyl	Sigma	381586
IAA	Sigma	I3750

REAGENT or RESOURCE	SOURCE	IDENTIFIER
Software and Algorithms		
MetaMorph	Molecular Devices	https://www.moleculardevices.com/products/cellular-imaging-systems/acquisition-and-analysis-software/metamorph-microscopy
MatLab	MathWorks	https://www.mathworks.com/products/matlab.html

Supplementary Material

Refer to Web version on PubMed Central for supplementary material.

ACKNOWLEDGEMENTS

Reference List

1. Musacchio A, and Desai A (2017). A Molecular View of Kinetochore Assembly and Function. Biology (Basel) 6.

2. Biggins S (2013). The composition, functions, and regulation of the budding yeast kinetochore. Genetics 194, 817–846. [PubMed: 23908374]

3. Salmon ED, and Bloom K (2017). Tension sensors reveal how the kinetochore shares its load. Bioessays.

4. Suzuki A, Badger BL, Haase J, Ohashi T, Erickson HP, Salmon ED, and Bloom K (2016). How the kinetochore couples microtubule force and centromere stretch to move chromosomes. Nature cell biology 18, 382–392. [PubMed: 26974660]

5. Akiyoshi B, Sarangapani KK, Powers AF, Nelson CR, Reichow SL, Arellano-Santoyo H, Gonen T, Ranish JA, Asbury CL, and Biggins S (2010). Tension directly stabilizes reconstituted kinetochore-microtubule attachments. Nature 468, 576–579. [PubMed: 21107429]

6. Powers AF, Franck AD, Gestaut DR, Cooper J, Gracyzk B, Wei RR, Wordeman L, Davis TN, and Asbury CL (2009). The Ndc80 kinetochore complex forms load-bearing attachments to dynamic microtubule tips via biased diffusion. Cell 136, 865–875. [PubMed: 19269365]

7. Cheeseman IM, Chappie JS, Wilson-Kubalek EM, and Desai A (2006). The conserved KMN network constitutes the core microtubule-binding site of the kinetochore. Cell 127, 983–997. [PubMed: 17129783]

8. DeLuca JG, Gall WE, Ciferri C, Cimini D, Musacchio A, and Salmon ED (2006). Kinetochore microtubule dynamics and attachment stability are regulated by Hec1. Cell 127, 969–982. [PubMed: 17129782]

9. Ciferri C, Pasqualato S, Screpanti E, Varetti G, Santaguida S, Dos Reis G, Maiolica A, Polka J, De Luca JG, De Wulf P, et al. (2008). Implications for kinetochore-microtubule attachment from the structure of an engineered Ndc80 complex. Cell 133, 427–439. [PubMed: 18455984]

10. DeLuca KF, Lens SM, and DeLuca JG (2011). Temporal changes in Hec1 phosphorylation control kinetochore-microtubule attachment stability during mitosis. Journal of cell science 124, 622–634. [PubMed: 21266467]

11. Akiyoshi B, Nelson CR, Ranish JA, and Biggins S (2009). Analysis of Ipl1-mediated phosphorylation of the Ndc80 kinetochore protein in Saccharomyces cerevisiae. Genetics 183, 1591–1595. [PubMed: 19822728]

12. Nogales E, and Ramey VH (2009). Structure-function insights into the yeast Dam1 kinetochore complex. Journal of cell science 122, 3831–3836. [PubMed: 19889968]

13. Hofmann C, Cheeseman IM, Goode BL, McDonald KL, Barnes G, and Drubin DG (1998). Saccharomyces cerevisiae Duo1p and Dam1p, novel proteins involved in mitotic spindle function. The Journal of cell biology 143, 1029–1040. [PubMed: 9817759]

14. Li Y, Bachant J, Alcasabas AA, Wang Y, Qin J, and Elledge SJ (2002). The mitotic spindle is required for loading of the DASH complex onto the kinetochore. Genes & development 16, 183–197. [PubMed: 11799062]

15. Janke C, Ortiz J, Tanaka TU, Lechner J, and Schiebel E (2002). Four new subunits of the Dam1-Duo1 complex reveal novel functions in sister kinetochore biorientation. The EMBO journal 21, 181–193. [PubMed: 11782438]

16. Enquist-Newman M, Cheeseman IM, Van Goor D, Drubin DG, Meluh PB, and Barnes G (2001). Dad1p, third component of the Duo1p/Dam1p complex involved in kinetochore function and mitotic spindle integrity. Molecular biology of the cell 12, 2601–2613. [PubMed: 11553702]

17. Tanaka TU, and Desai A (2008). Kinetochore-microtubule interactions: the means to the end. Current opinion in cell biology 20, 53–63. [PubMed: 18182282]

18. Miranda JJ, De Wulf P, Sorger PK, and Harrison SC (2005). The yeast DASH complex forms closed rings on microtubules. Nature structural & molecular biology 12, 138–143.

19. Kim JO, Zelter A, Umbreit NT, Bollozos A, Riffle M, Johnson R, MacCoss MJ, Asbury CL, and Davis TN (2017). The Ndc80 complex bridges two Dam1 complex rings. Elife 6.

20. Slep KC, and Vale RD (2007). Structural basis of microtubule plus end tracking by XMAP215, CLIP-170, and EB1. Molecular cell 27, 976–991. [PubMed: 17889670]

21. Miller MP, Asbury CL, and Biggins S (2016). A TOG Protein Confers Tension Sensitivity to Kinetochore-Microtubule Attachments. Cell 165, 1428–1439. [PubMed: 27156448]

22. Tang NH, Takada H, Hsu KS, and Toda T (2013). The internal loop of fission yeast Ndc80 binds Alp7/TACC-Alp14/TOG and ensures proper chromosome attachment. Molecular biology of the cell 24, 1122–1133. [PubMed: 23427262]

23. Sarangapani KK, Akiyoshi B, Duggan NM, Biggins S, and Asbury CL (2013). Phosphoregulation promotes release of kinetochores from dynamic microtubules via multiple mechanisms. Proceedings of the National Academy of Sciences of the United States of America 110, 7282–7287. [PubMed: 23589891]

24. Tien JF, Umbreit NT, Gestaut DR, Franck AD, Cooper J, Wordeman L, Gonen T, Asbury CL, and Davis TN (2010). Cooperation of the Dam1 and Ndc80 kinetochore complexes enhances microtubule coupling and is regulated by aurora B. The Journal of cell biology 189, 713–723. [PubMed: 20479468]

25. Kashina AS, Baskin RJ, Cole DG, Wedaman KP, Saxton WM, and Scholey JM (1996). A bipolar kinesin. Nature 379, 270–272. [PubMed: 8538794]

26. Hildebrandt ER, and Hoyt MA (2000). Mitotic motors in Saccharomyces cerevisiae. Biochimica et biophysica acta 1496, 99–116. [PubMed: 10722880]

27. Hoyt MA, He L, Loo KK, and Saunders WS (1992). Two Saccharomyces cerevisiae kinesin-related gene products required for mitotic spindle assembly. The Journal of cell biology 118, 109–120. [PubMed: 1618897]

28. Roostalu J, Hentrich C, Bieling P, Telley IA, Schiebel E, and Surrey T (2011). Directional switching of the kinesin Cin8 through motor coupling. Science 332, 94–99. [PubMed: 21350123]

29. Shapira O, and Gheber L (2016). Motile properties of the bi-directional kinesin-5 Cin8 are affected by phosphorylation in its motor domain. Sci Rep 6, 25597. [PubMed: 27216310]

30. Straight AF, Sedat JW, and Murray AW (1998). Time-lapse microscopy reveals unique roles for kinesins during anaphase in budding yeast. The Journal of cell biology 143, 687–694. [PubMed: 9813090]

31. Tytell JD, and Sorger PK (2006). Analysis of kinesin motor function at budding yeast kinetochores. The Journal of cell biology 172, 861–874. [PubMed: 16533946]

32. Geiser JR, Schott EJ, Kingsbury TJ, Cole NB, Totis LJ, Bhattacharyya G, He L, and Hoyt MA (1997). Saccharomyces cerevisiae genes required in the absence of the CIN8-encoded spindle

motor act in functionally diverse mitotic pathways. Molecular biology of the cell 8, 1035–1050. [PubMed: 9201714]

33. He X, Rines DR, Espelin CW, and Sorger PK (2001). Molecular analysis of kinetochore-microtubule attachment in budding yeast. Cell 106, 195–206. [PubMed: 11511347]

34. Demirel PB, Keyes BE, Chaterjee M, Remington CE, and Burke DJ (2012). A redundant function for the N-terminal tail of Ndc80 in kinetochore-microtubule interaction in Saccharomyces cerevisiae. Genetics 192, 753–756. [PubMed: 22851650]

35. Petrovic A, Pasqualato S, Dube P, Krenn V, Santaguida S, Cittaro D, Monzani S, Massimiliano L, Keller J, Tarricone A, et al. (2010). The MIS12 complex is a protein interaction hub for outer kinetochore assembly. The Journal of cell biology 190, 835–852.

36. Akiyoshi B, Nelson CR, Ranish JA, and Biggins S (2009). Quantitative proteomic analysis of purified yeast kinetochores identifies a PP1 regulatory subunit. Genes & development 23, 2887–2899. [PubMed: 19948764]

37. Gonen S, Akiyoshi B, Iadanza MG, Shi D, Duggan N, Biggins S, and Gonen T (2012). The structure of purified kinetochores reveals multiple microtubule-attachment sites. Nature structural & molecular biology 19, 925–929.

38. Pearson CG, Maddox PS, Zarzar TR, Salmon ED, and Bloom K (2003). Yeast kinetochores do not stabilize Stu2p-dependent spindle microtubule dynamics. Molecular biology of the cell 14, 4181–4195. [PubMed: 14517328]

39. Joglekar AP, Bouck DC, Molk JN, Bloom KS, and Salmon ED (2006). Molecular architecture of a kinetochore-microtubule attachment site. Nature cell biology 8, 581–585. [PubMed: 16715078]

40. Aravamudhan P, Felzer-Kim I, Gurunathan K, and Joglekar AP (2014). Assembling the Protein Architecture of the Budding Yeast Kinetochore-Microtubule Attachment using FRET. Current biology : CB 24, 1437–1446. [PubMed: 24930965]

41. Haase J, Mishra PK, Stephens A, Haggerty R, Quammen C, Taylor RM, 2nd, Yeh E, Basrai MA, and Bloom K (2013). A 3D map of the yeast kinetochore reveals the presence of core and accessory centromere-specific histone. Current biology : CB 23, 1939–1944. [PubMed: 24076245]

42. Umbreit NT, Miller MP, Tien JF, Ortola JC, Gui L, Lee KK, Biggins S, Asbury CL, and Davis TN (2014). Kinetochores require oligomerization of Dam1 complex to maintain microtubule attachments against tension and promote biorientation. Nature communications 5, 4951.

43. Lampert F, Mieck C, Alushin GM, Nogales E, and Westermann S (2013). Molecular requirements for the formation of a kinetochore-microtubule interface by Dam1 and Ndc80 complexes. The Journal of cell biology 200, 21–30. [PubMed: 23277429]

44. Maure JF, Komoto S, Oku Y, Mino A, Pasqualato S, Natsume K, Clayton L, Musacchio A, and Tanaka TU (2011). The Ndc80 loop region facilitates formation of kinetochore attachment to the dynamic microtubule plus end. Current biology : CB 21, 207–213. [PubMed: 21256019]

45. Asbury CL (2017). Anaphase A: Disassembling Microtubules Move Chromosomes toward Spindle Poles. Biology (Basel) 6.

46. Gheber L, Kuo SC, and Hoyt MA (1999). Motile properties of the kinesin-related Cin8p spindle motor extracted from Saccharomyces cerevisiae cells. The Journal of biological chemistry 274, 9564–9572. [PubMed: 10092642]

47. Rosenberg JS, Cross FR, and Funabiki H (2011). KNL1/Spc105 recruits PP1 to silence the spindle assembly checkpoint. Current biology : CB 21, 942–947. [PubMed: 21640906]

48. Liu D, Vleugel M, Backer CB, Hori T, Fukagawa T, Cheeseman IM, and Lampson MA (2010). Regulated targeting of protein phosphatase 1 to the outer kinetochore by KNL1 opposes Aurora B kinase. The Journal of cell biology 188, 809–820. [PubMed: 20231380]

49. Hafner J, Mayr MI, Mockel MM, and Mayer TU (2014). Pre-anaphase chromosome oscillations are regulated by the antagonistic activities of Cdk1 and PP1 on Kif18A. Nature communications 5, 4397.

50. Kim H, and Stumpff J, biorxiv, (https://doi.org/10.1101/304147)

51. Nishimura K, Fukagawa T, Takisawa H, Kakimoto T, and Kanemaki M (2009). An auxin-based degron system for the rapid depletion of proteins in nonplant cells. Nature methods 6, 917–922. [PubMed: 19915560]

52. Suzuki A, Badger BL, and Salmon ED (2015). A quantitative description of Ndc80 complex linkage to human kinetochores. Nature communications 6, 8161.

53. Gupta A, Evans RK, Koch LB, Littleton AJ, and Biggins S (2018). Purification of kinetochores from the budding yeast Saccharomyces cerevisiae. Methods Cell Biol 144, 349–370. [PubMed: 29804677]

Highlights

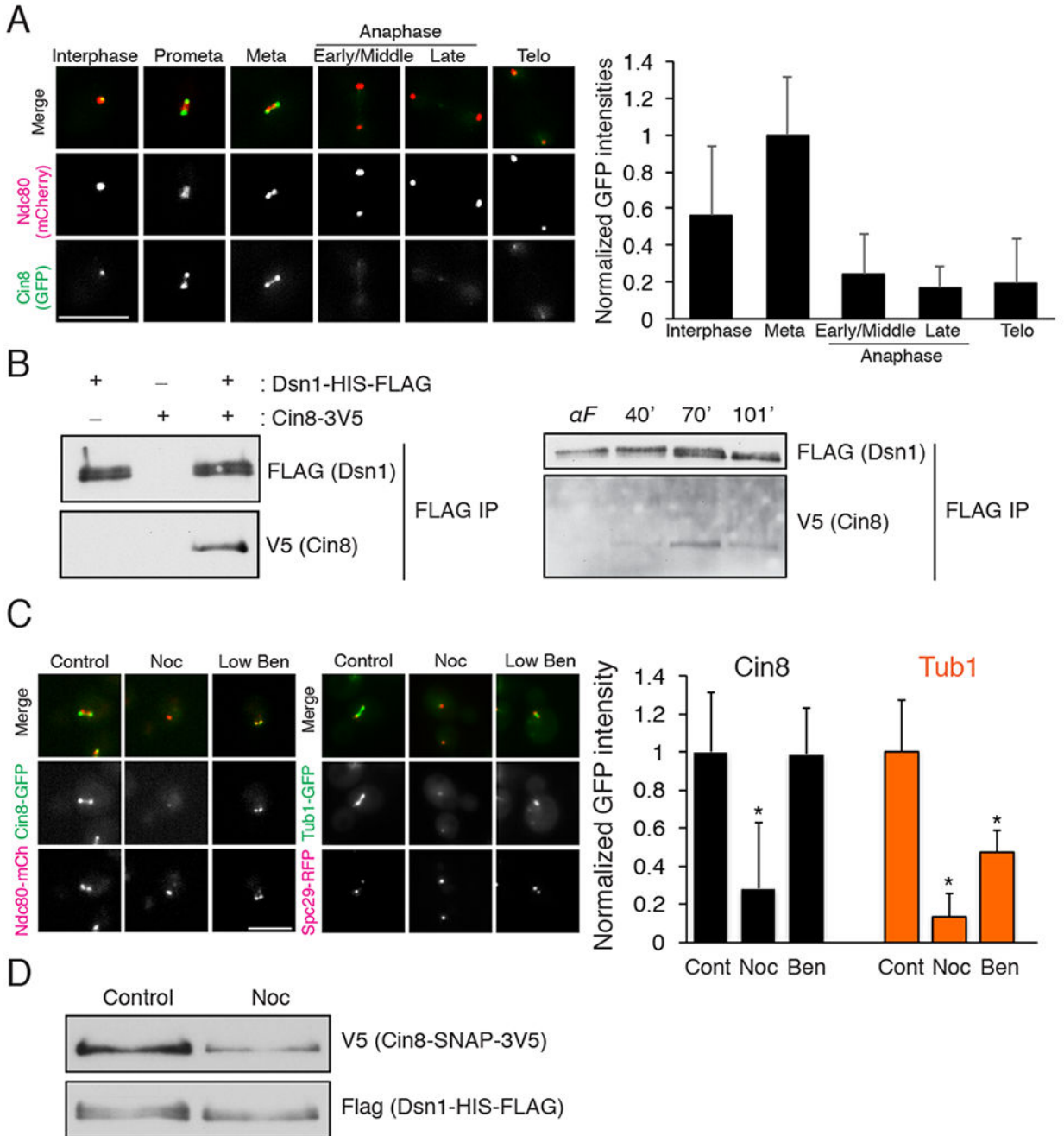1. The microtubule-based motor Cin8 is required to build tension in the Ndc80 complex

2. Cin8 kinetochore localization depends on kinetochore MTs, Ndc80 and Daml complexes.

3. Cin8 binds PP1 and is localized near the N-terminal tail of Ndc80 at kinetochores.

4. *cin8-RAKA* mutant induces a loss of tension at Ndc80 and a severe mitotic delay.

Figure 1. Cin8 localizes to kinetochores in cell cycle-dependent manner.
(A) Representative images of Cin8-GFP and Ndc80-mCherry throughout the cell cycle (left). The plot of normalized GFP intensity at kinetochores throughout the cell cycle (right). The signal intensity was normalized for the mean values of metaphase. (B) Dsn1-His-Flag was immunoprecipitated from asynchronously growing yeast cells expressing Dsn1-His-Flag, Cin8-3V5, or Dsn1-His-Flag/Cin8-3V5 (left) or from Dsn1-His-Flag/Cin8-3V5 cells that were synchronized in G1 (using α-factor), released and harvested after 0, 40, 70, and 101 min (right). The levels of Cin8 that associate with kinetochores was analyzed by

immunoblotting. See also Figure S1. (C) Representative images of Cin8-GFP and Ndc80-mCherry in control, nocodazole (Noc), or low dose benomyl (Low Ben) treated cells (left). The plot of normalized GFP intensity (right). The signal intensity was normalized for the mean values of control for either Cin8 or tubulin (Tub1). All values were mean ± SD. n > 80 individual kinetochores for each experiment. * p < 0.05 (t-test). Scale bars were 5 μm. (D) Kinetochores were isolated by immunoprecipitation of Dsn1-His-Flag from asynchronously growing yeast cells expressing Cin8-Snap-3V5 that were treated with or without nocodazole (noc) for 15 min. The levels of Cin8 that associate with kinetochores were detected by immunoblotting.
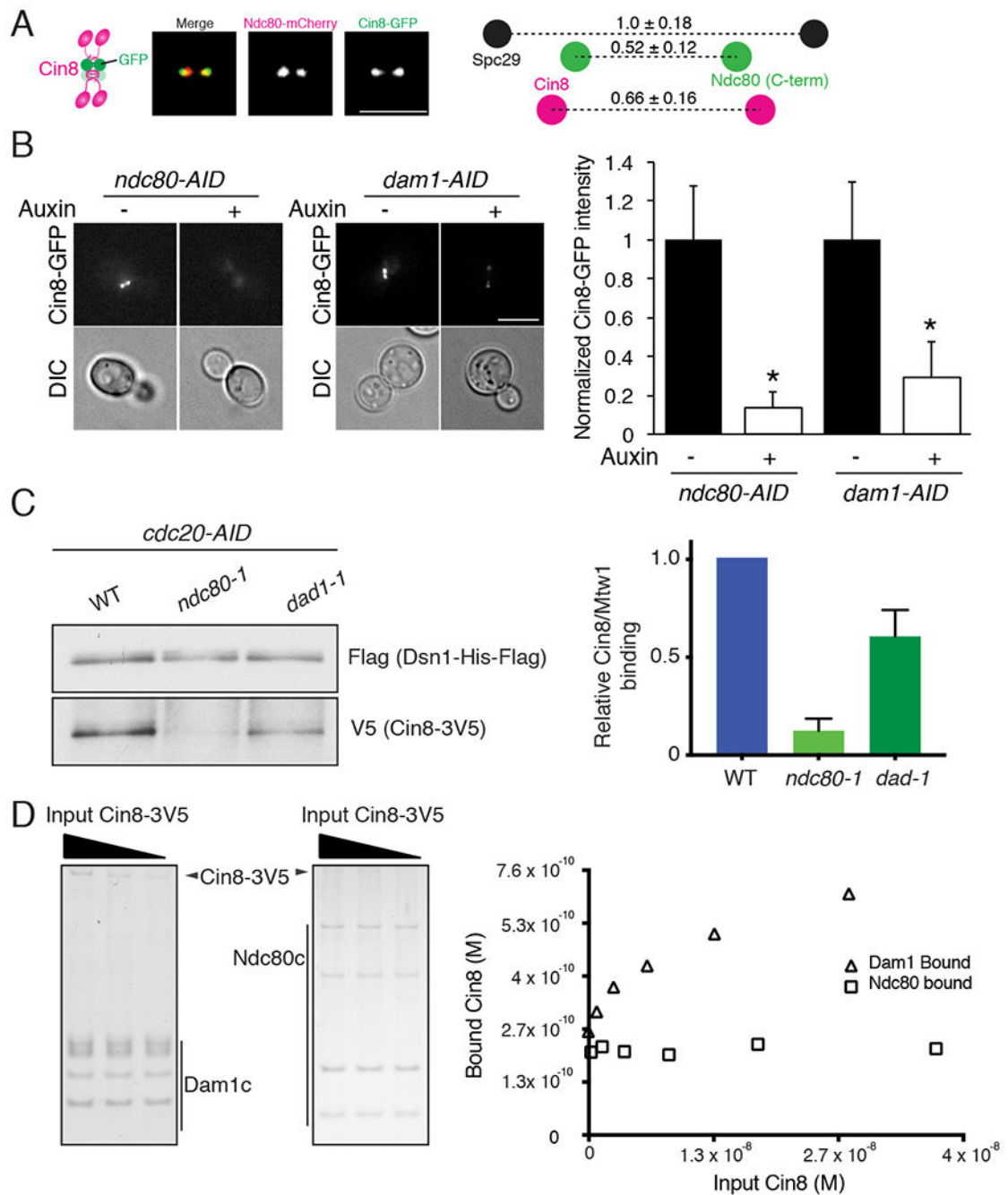
Figure 2. The Ndc80 and Dam1 complexes are required for Cin8 kinetochore localization.
(A) Representative images of Cin8-GFP and Ndc80-mCherry at metaphase (left). The separation between sister Cin8, Ndc80, and Spc29 clusters was obtained from cells expressing Spc29-RFP and Cin8-GFP, or Spc29-RFP and Ndc80-GFP. The separation was normalized for the separation values of Spc29-Spc29 (right). Scale bars are 2.5 μm. (B) Representative images of Cin8-GFP at metaphase in control, Ndc80 depleted cells, and Dam1 depleted cells (left). The plot of normalized GFP intensity (right). The signal intensity was normalized for the mean values of each control. All values are mean ± SD. n > 80

individual kinetochores for each experiment. * p < 0.05 (t-test). Scale bars are 5 μm. (C) Kinetochores were purified via immunoprecipitation of Dsnl-His-Flag from WT, *ndc80-1* or *dad1-1* cells that had been shifted to 37 °C for 2 hours. The levels of Cin8-3V5 that co-purify with kinetochores were analyzed by immunoblotting (left) and quantified by normalizing the intensity relative to the levels of the core kinetochore protein Mtwl (right). (D) Immunoprecipitation with anti-V5 antibody from solution containing purified Cin8-3V5 and Dam1 complex, or Cin8-3V5 and Ndc80 complex (left, See Methods). The plot of Cin8 bound to Ndc80 or Dam1 versus input Cin8 (right).
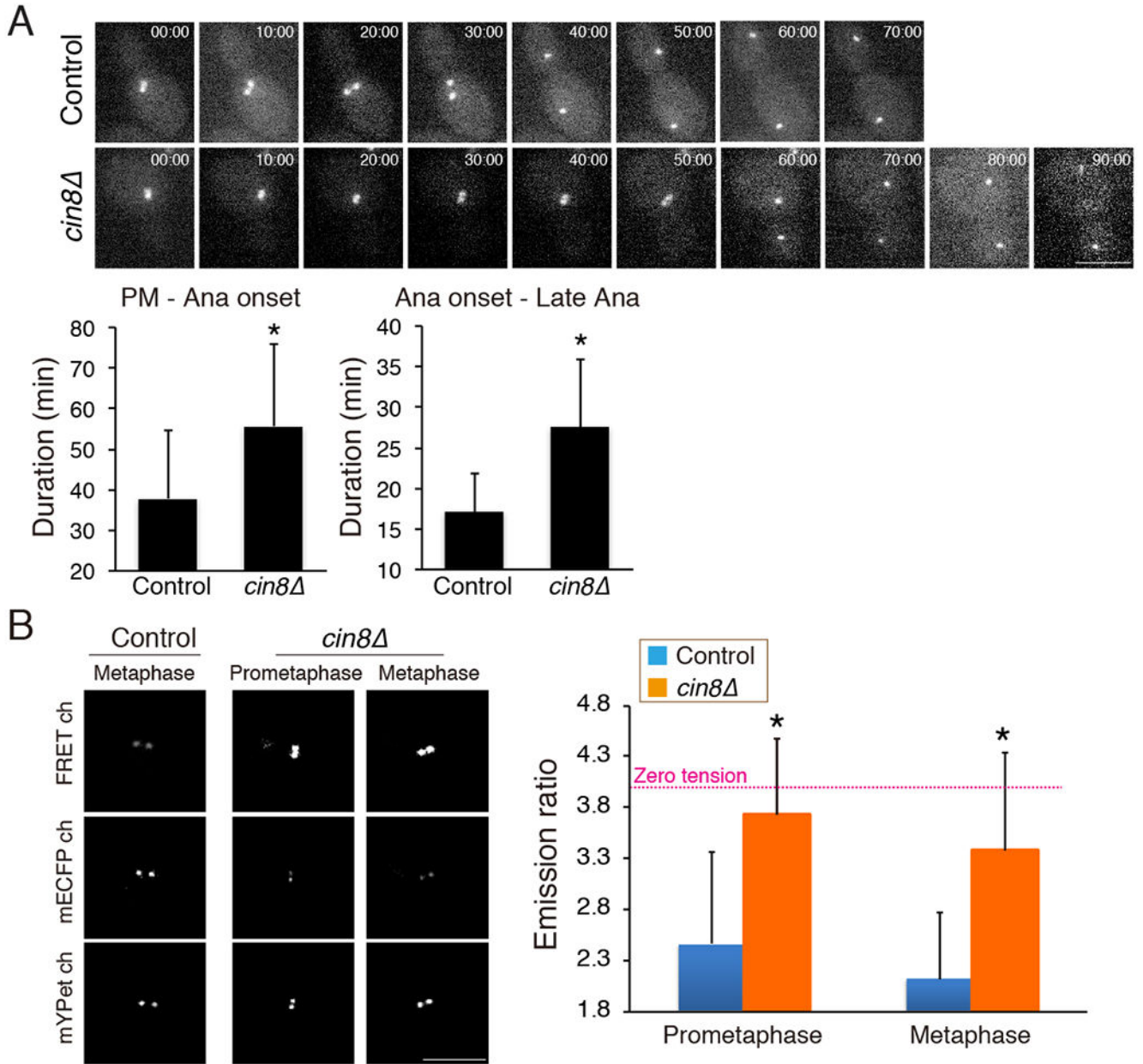
Figure 3. Cin8 is essential for producing proper tension at Ndc80.
(A) Representative time-lapse images of control and Cin8 deletion cells (top). The mean duration between prometaphase (PM) and Anaphase onset (Ana onset), and between Ana onset and late anaphase (Late Ana) (bottom). Mitotic stages are determined by sister kinetochore separations (K-K) and cellular bud neck [4]. K-K < 700 nm (Prometaphase), 700 nm < K-K < 1000 nm (Metaphase), K-K > 1000 nm (Anaphase), and Late anaphase is just before Telophase. n = 45 (control) and 24 (Cin8 deletion). (B) Representative FRET images of control and Cin8 deletion cells at prometaphase and metaphase (left). The mean FRET emission ratio in each condition (right). All values are mean ± SD. n > 100 individual kinetochores for each experiment. * p < 0.05 (t-test). Scale bars are 5 μm. See also Figure S2.
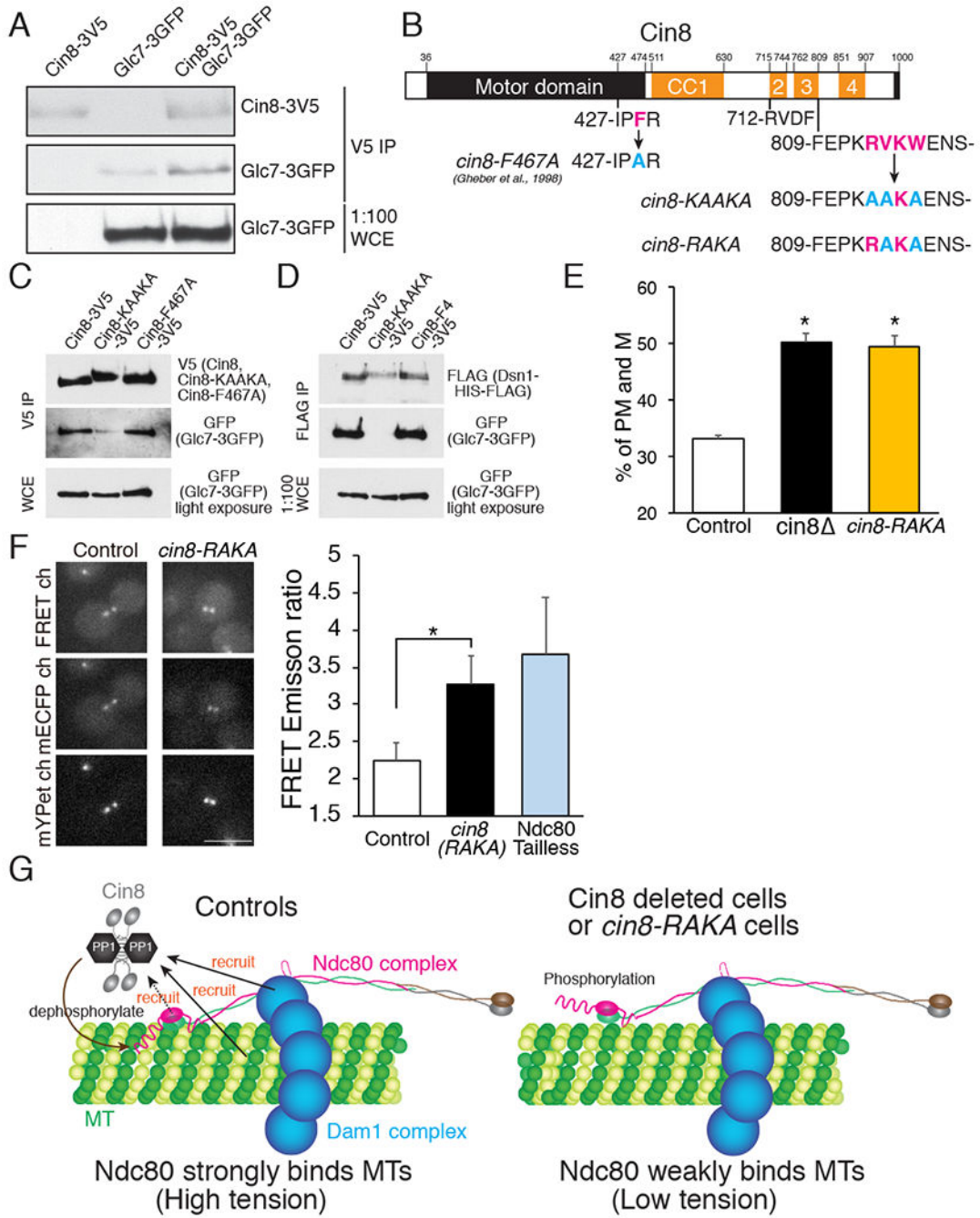
Figure 4. Cin8 binds to PP1 to promote mitotic progression and tension at Ndc80.
(A) Cin8 was immunoprecipitated from cells expressing Cin8-3V5, Glc7-3GFP, or
Cin8-3V5/Glc7-3GFP and the levels of associated Glc7 were analyzed by immunoblotting.
(B) Schematic of the Cin8 protein, which has a motor domain (black) and four coiled coil
(CC) domains (orange). Cin8 has a PP1 binding motif between CC3 and CC4 domains, and
two mutants designed to abolish PP1 binding are indicated. The motor mutant, *cin8-F467A*
[46], is also indicated. Note that the authors in [46] used the original annotated Cin8, which
started 38 amino-acids upstream of the actual start codon. (C) Cin8, *cin8-KAAKA* or *cin8-*

F467A were immunoprecipitated from cells that were also expressing Glc7-3GFP and the levels of co-purifying Glc7 were analyzed by immunoblotting. (D) Kinetochores were purified via Dsn1-His-Flag from cells expressing Cin8-3V5, *cin8-KAAKA-3V5*, or *cin8-F467A-4V5*, and the levels of associated Glc7 were analyzed by immunoblotting. (E) Percentage of prometaphase (PM) and metaphase (M) cells in control, *cin8* cells, and *cin8-RAKA* mutant cells. (F) Representative FRET images of control and cin8-RAKA mutant cells (left). The mean FRET emission ratio in condition left (right). All values were mean ± SD. n > 100 individual kinetochores for each experiment. * p < 0.05 (t-test). Scale bars were 5 μm. See also Figure S3. (G) Schematic models of how yeast kinesin-5 regulates proper force production at the microtubule binding domains of Ndc80. In wild type cells, Cin8 recruits PP1 to kinetochores during early mitosis in manner that requires microtubules, Ndc80 and Dam1 complexes. This leads to PP1 dephosphorylation of the Ndc80 N-terminus to strengthen its attachment to microtubules and to produce force for proper mitotic progression. In Cin8 depleted cells, kinetochore-microtubule attachments are weak because the N-terminal tail of Ndc80 remains phosphorylated due to the loss of PP1.